Case of Aggressive Posterior Retinopathy of Prematurity with Atypical Neovascular Growth

Fibrovascular proliferation in eyes with retinopathy of prematurity (ROP) usually, but not always, appears at the junction of the vascularized and nonvascularized retina.[1] Aggressive posterior ROP (AP-ROP) occurs in the posterior retina and progresses rapidly to total retinal detachment.[2] We report an atypical case of AP-ROP in which the neovascularization developed in the posterior retina around the optic disc.

Case Report

A female infant was born at 30 weeks' gestation (birth weight, 1670 g) with severe persistent pulmonary hypertension from prolonged premature rupture of the membranes and oligohydramnios. She was treated with nitric oxide (NO) inhalation for 28 days. At 33 weeks postmenstrual age, an ophthalmoscopic examination identified initial signs of zone I AP-ROP bilaterally, including marked dilation and tortuosity of the posterior pole vessels (zone I, stage 1 ROP with plus disease).

Argon laser photocoagulation was performed (duration, 300–400 ms; power, 300–400 mW; 3751 shots OD, 3658 shots OS) under intravenous sedation (fentanyl) with topical anesthesia. However, fibrovascular proliferation and retinal detachment developed bilaterally in the posterior retina around the optic disc 1 week postoperatively (Fig. 1a, b). The patient underwent vitrectomy with lensectomy as a secondary treatment at 35 weeks postmenstrual age. The retina was reattached and the ROP stabilized in the left eye, but the fibrovascular tissue regrew from the posterior retina of the right eye (Fig. 1c). A second vitrectomy stabilized the ROP in that eye (Fig. 1d).

Immunohistochemistry of the fibrovascular tissue collected during vitrectomy was strongly positive for factor VIII over a wide area and locally positive for vimentin but negative for glial fibrillary acidic protein. These findings suggested that the tissue consisted mainly of vascular endothelial cells (Fig. 2).

Comments

We report the successful surgical results of early vitrectomy for AP-ROP.[3] Our findings suggest that when neovascularization develops only at the peripheral end of the developing vessels, the retina can be reattached by removing the vitreous framework around the fibrovascular tissue and the vitreous base. These procedures reduce the tractional forces of the fibrovascular tissue and suppress neovascular growth. Residual vitreous gel did not affect the retinal reattachment, and a regrowth of neovascularization was not observed in a previous study.[3]

In our case, the neovascularization that developed in the posterior retina could have grown along the residual vitreous gel on the retinal surface and around the optic disc. This tissue could not be completely removed during the initial vitrectomy. In cases such as this, another vitrectomy to peel the residual vitreous gel can lead to retinal reattachment, which worked well in our case.

Jpn J Ophthalmol
Vol 52: 407–425, 2008

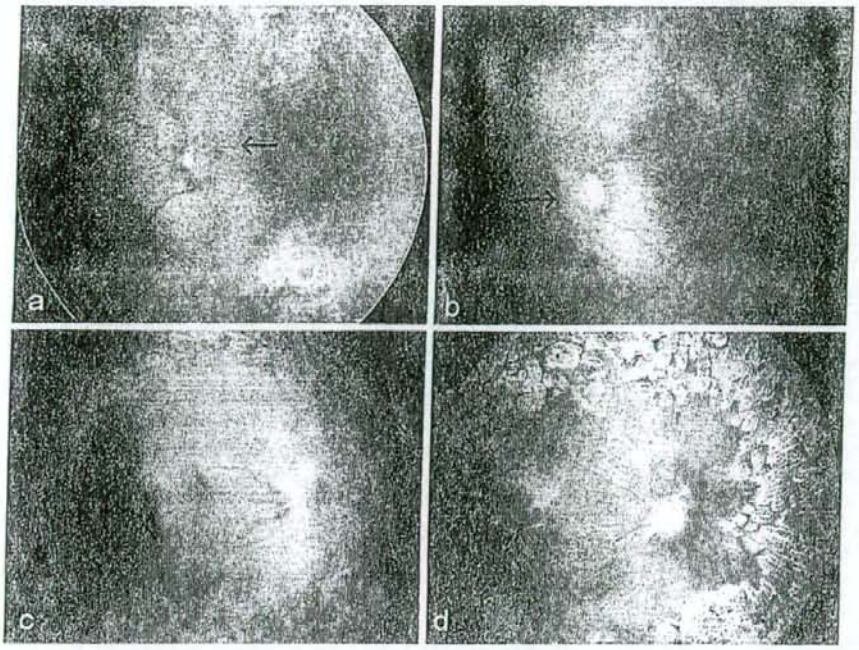

Figure 1a–d. Preoperative and postoperative fundus photographs of eyes with aggressive posterior retinopathy of prematurity (ROP). **a** Preoperative fundus image of the right eye. **b** Preoperative fundus image of the left eye. Fibrovascular proliferation and tractional retinal detachment (*arrows*) are present nasally in the posterior retina of both eyes. **c** Two weeks after the initial vitrectomy, the neovascularization has regrown and formed a fibrous membrane and tractional retinal detachment in the right eye. **d** The retina is reattached and the ROP is stabilized after additional vitrectomy of the right eye.

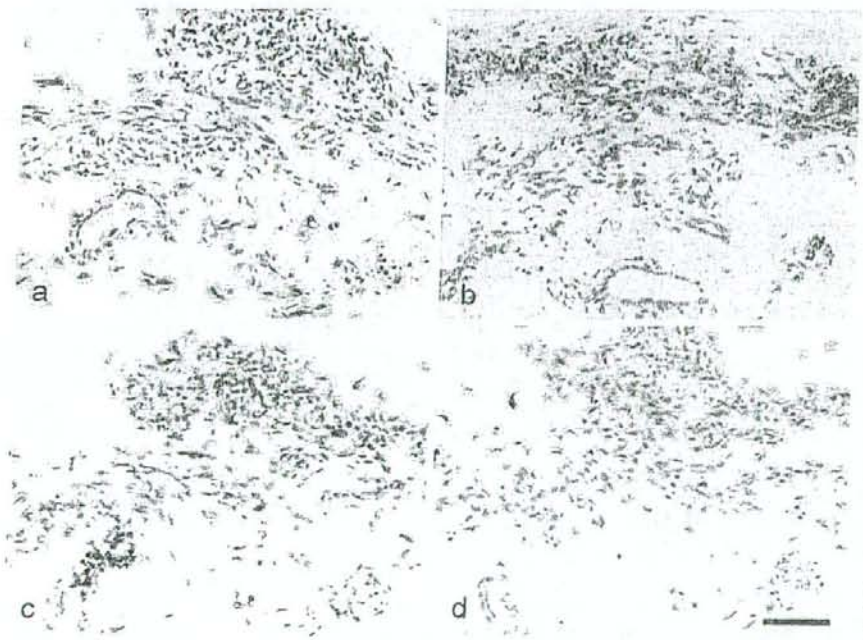

Figure 2a–d. Pathology and immunohistochemistry of the fibrovascular tissue obtained during the second vitrectomy. H&E staining (**a**) and immunohistochemistry with antibodies against factor VIII (**b**), vimentin (**c**), and glial fibrillary acidic protein (**d**). Immunohistochemistry showed that the fibrovascular tissue was strongly positive for factor VIII over a wide area (**b**), and was locally positive for vimentin (**c**) but negative for glial fibrillary acidic protein (**d**). These findings suggest that the tissue was composed of vascular endothelial cells (scale bar = 50 μm).

In eyes with AP-ROP, a flat network of neovascularization arises from the peripheral terminals of the developing vessels as in classical ROP, even though vascular shunts occur in the vascularized retina. However, in our patient, the fibrovascular proliferation developed atypically in the posterior retina around the optic disc. Except for the prolonged NO inhalation, systemic therapies including oxygen administration and laser application might not contribute

to the atypical growth of the neovascularization. While NO is known to derive vasodilatation and up-regulates regional basal blood flow,[4] it also activates angiogenic cell migration and proliferation-inducing factors, including fibroblast growth factor 2 and vascular endothelial growth factor.[5] Because retinal angiogenesis is ongoing in premature infants, NO might have contributed to the atypical neovascularization near the optic disc in our patient.

In animal models of oxygen-induced retinopathy, neovascularization induced by obliteration of the immature capillaries also develops from the optic disc and posterior retina.[6] Because AP-ROP develops in the posterior retinal area, including zone I, this suggests that immature capillaries may be widely present, and neovascularization arises from the retina near the optic disc. Capillary nonperfusion in vascularized retinas has been identified in eyes with threshold ROP.[7] Thus, there might be a much wider area of nonperfusion in the posterior retina in eyes with AP-ROP, which should be studied using fluorescein angiography.

Acknowledgments. This work was supported by grants for research on sensory disorders from the Ministry of Health, Labour and Welfare, Japan.

Key Words: aggressive posterior retinopathy of prematurity, fibrovascular proliferation, photocoagulation, regrowth, vitrectomy

Miina Hiraoka, Sachiko Nishina, Atsuko Nakagawa, Kentaro Matsuoka, and Noriyuki Azuma
Department of Ophthalmology, National Center for Child Health and Development, Tokyo, Japan

Received: December 11, 2007 / Accepted: April 23, 2008
Correspondence to: Noriyuki Azuma, Department of Ophthalmology, National Center for Child Health and Development, 2-10-1 Okura, Setagaya-ku, Tokyo 157-8535, Japan
e-mail: azuma-n@ncchd.go.jp

DOI 10.1007/s10384-008-0557-3

References

1. Foos RY. Retinopathy of prematurity. Pathologic correlation of clinical stages. Retina 1987;7:260–276.
2. International Committee for the Classification of Retinopathy of Prematurity. The international classification of retinopathy of prematurity revisited. Arch Ophthalmol 2005;123:991–999.
3. Azuma N, Ishikawa K, Hama Y, Hiraoka M, Suzuki Y, Nishina S. Early vitreous surgery for aggressive posterior retinopathy of prematurity. Am J Ophthalmol 2006;142:636–643.
4. Gross SS, Wolin MS. Nitric oxide: pathophysiological mechanisms. Annu Rev Physiol 1995;57:737–769.
5. Ziche M, Morbidelli L. Nitric oxide and angiogenesis. J Neurooncol 2000;50:139–148.
6. McLeod DS, D'Anna SA, Lutty GA. Clinical and histopathological features of canine oxygen-induced proliferative retinopathy. Invest Ophthalmol Vis Sci 1998;39:1918–1932.
7. Schulenburg WE, Tsanaktsidis G. Variations in the morphology of retinopathy of prematurity in extremely low birthweight infants. Br J Ophthalmol 2004;88:1500–1503.

Graefes Arch Clin Exp Ophthalmol (2008) 246:453–455
DOI 10.1007/s00417-007-0741-z

CASE REPORT

Exudative retinal detachment following cataract surgery in Hallermann-Streiff syndrome

Sachiko Nishina · Yumi Suzuki · Noriyuki Azuma

Received: 7 September 2007 / Revised: 17 November 2007 / Accepted: 27 November 2007 / Published online: 12 January 2008

Abstract
Purpose To report two cases of Hallermann-Streiff syndrome with exudative retinal detachment after cataract surgery.
Methods Case report.
Results Four eyes of two patients with Hallermann-Streiff syndrome developed exudative retinal detachments after lensectomy and anterior vitrectomy at 2 and 4 months of age. Both patients had extreme microphthalmia. The exudative retinal detachment regressed spontaneously in three of the four eyes; however, one eye required subscleral sclerectomy. In one patient, the best-corrected visual acuity was 20/200 at 3 years of age; the other patient had good fixation and following behavior in each eye at 1 year of age.
Conclusions Early surgery to treat congenital cataracts in extremely microphthalmic eyes associated with the Hallermann-Streiff syndrome may induce exudative retinal detachment. However, the retinal detachments tend to regress and may not cause severe visual impairment.

Keywords Hallermann-Streiff syndrome · Exudative retinal detachment · Cataract surgery · Microphthalmos

Introduction

The Hallermann-Streiff syndrome is a rare complex of developmental abnormalities characterized by dyscephaly with bird face, beak nose and micrognathia, dental anomalies, hypotrichosis, skin atrophy, microphthalmia, congenital cataracts, and proportionate dwarfism [1]. Most cases are sporadic, and the etiology is unknown. Various ocular findings and fundus anomalies have been reported, including vitreous degeneration, retinal folds, coloboma, and Coats' disease; however, a few reports have described detailed fundus changes after cataract surgery [2–4]. To our knowledge, this is the first report on the development of exudative retinal detachments after cataract surgery in four microphthalmic eyes of two patients with the Hallermann-Streiff syndrome.

Case report

Patient 1, a 1-month-old Japanese male infant, referred with a diagnosis of bilateral congenital cataracts and microphthalmia. He had the typical features of the Hallermann-Streiff syndrome, including dyscephaly with beak nose and micrognathia, dental anomalies, hypotrichosis, skin atrophy, and proportionate dwarfism (Fig. 1a). A slit-lamp examination revealed total cataracts, a microcornea (corneal diameter, 7×7.5 mm OD and 8×8.5 mm OS), a shallow anterior chamber, posterior synechiae, and poor pupil dilation in both eyes. Ultrasonography showed bilateral microphthalmia (axial length, 13 mm OD and 14 mm OS) but no other posterior segment anomalies. Lensectomy and anterior vitrectomy via the limbal approach using a 25-gauge surgical system was performed in both eyes at 2 months of age. No intraoperative or postoperative complications developed except for transient corneal edema. Ophthalmoscopy identified small retinal folds between the disc and fovea in both eyes. The aphakic eyes were corrected with glasses, and both eyes developed fixation and following behavior.

The authors have no proprietary interest in any aspect of this report.

S. Nishina (✉) · Y. Suzuki · N. Azuma
Department of Ophthalmology,
National Center for Child Health and Development,
2-10-1 Ohkura, Setagaya-ku,
Tokyo 157-8535, Japan
e-mail: nishina-s@ncchd.go.jp

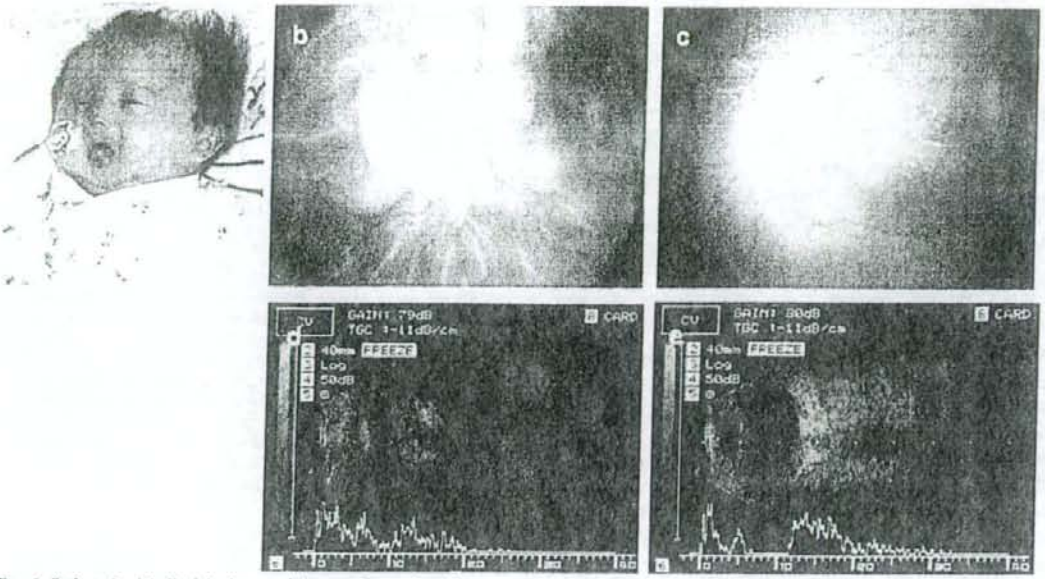

Fig. 1 Patient 1. (a) Facial characteristics at 2 months of age. Bilateral exudative retinal detachments at 7 months of age. The right eye (b) has the more severe retinal detachment and requires subscleral sclerectomy. The left eye (c) also has an exudative retinal detachment that regressed spontaneously. Ultrasonography shows both right eye (d) and left eye (e) have exudative retinal detachments with choroidal thickening

We examined the patient every month and then at 5 months after cataract surgery (7 months of age) when exudative retinal detachment developed in both eyes (Fig. 1b,c). Ultrasonography also showed bilateral exudative retinal detachment with choroidal thickening (Fig. 1d,e). The retinal detachment spontaneously regressed in the left eye, but progressed and did not regress in the right eye. Following behavior in the right eye deteriorated, and we performed a subscleral sclerectomy twice in that eye using 0.02% mitomycin C at 1 year 9 months and 2 years 4 months of age. The retinal detachment regressed, and at 3 years 5 months of age did not recur in either eye. The best-corrected visual acuity (BCVA) was 2/100 in the right eye and 20/200 in the left eye.

Patient 2, a 5-month-old Japanese female infant, referred with a diagnosis of bilateral retinal detachments after cataract surgery. She had undergone lensectomy and anterior vitrectomy at 4 months of age in another hospital. She exhibited the characteristic features of the Hallermann-Streiff syndrome, including dyscephaly with beak nose and micrognathia, dental anomalies, hypotrichosis, and proportionate dwarfism. A slit-lamp examination showed bilateral aphakia and a microcornea (corneal diameter, 7×7.5 mm OD and 8×8.5 mm OS). Ophthalmoscopy of both eyes showed exudative retinal detachments (Fig. 2). Ultrasonography showed bilateral microphthalmia (axial length, 13 mm OD and 14 mm OS) and retinal detachments with choroidal thickening. The retinal detachments spontaneous-

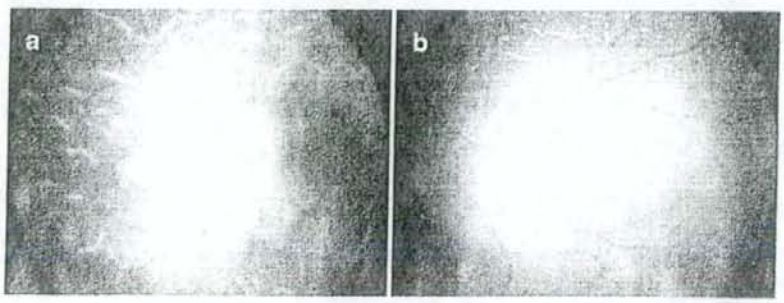

Fig. 2 Patient 2. Bilateral exudative retinal detachments at 1 years of age. The exudative retinal detachments regressed spontaneously in the right eye (a) and the left eye (b)

ly regressed in both eyes, and the patient had good fixation and following behavior with each eye at 1 year of age.

Discussion

These four eyes of two patients had severe microphthalmos and developed exudative retinal detachments after early surgery for congenital cataracts at 2 and 4 months of age. One of the four eyes required surgery; however, the retinal detachment regressed in three eyes, and the visual acuity was not severely impaired. This suggests that the extreme microphthalmic eye in the Hallermann-Streiff syndrome may have considerable scleral abnormalities that impede transscleral intraocular fluid outflow and result in congestion of the choroidal vein [5]. Early cataract surgery is supposed to induce hypotony, marked intraocular inflammation and transiently accelerate production of a protein-rich exudate. Intraocular fluid outflow may severely be resisted postoperatively and accumulated in choroid without venous drainage. It may possibly cause early onset of exudative retinal detachment in these eyes.

In this syndrome, spontaneous cataract absorption sometimes occurs, but results in deprivation amblyopia, iridocyclitis, and glaucoma [4, 6]. Although exudative retinal detachment tends to occur, it is preferable to perform early cataract surgery using less invasive procedures.

References

1. François J (1958) A new syndrome: Dyscephalia with bird face and dental anomalies, nanism, hypotrichosis, cutaneous atrophy, microphthalmia, and congenital cataract. Arch Ophthalmol 60:842–862
2. Cohen MM Jr (1991) Hallermann-Streiff syndrome: a review. Am J Med Genet 41:488–499
3. Newell SW, Hall BD, Anderson CW, Lim ES (1994) Hallermann-Streiff syndrome with Coats disease. J Pediatr Ophthalmol Strab 31:123–125
4. Hopkins DJ, Horan EC (1970) Glaucoma in the Hallermann-Streiff syndrome. Br J Ophthalmol 54:416–422
5. Ryan EA, Zwaan J, Chylack LT (1982) Nanophthalmos with uveal effusion. Clinical and embryologic considerations. Ophthalmology 89:1013–1017
6. Wolter JR, Jones DH (1965) Spontaneous cataract absorption in Hallermann-Streiff syndrome. Ophthalmologica 150:401–408

American Journal of Medical Genetics Part A 146A:2162–2163 (2008)

Research Letter

SOX10 Mutation in Waardenburg Syndrome Type II

Manami Iso,[1] Maki Fukami,[1] Reiko Horikawa,[2] Noriyuki Azuma,[3] Nobuko Kawashiro,[4] and Tsutomu Ogata[1]*

[1]Department of Endocrinology and Metabolism, National Research Institute for Child Health and Development, Tokyo, Japan
[2]Division of Endocrinology and Metabolism, National Center for Child Health and Development, Tokyo, Japan
[3]Division of Ophthalmology, National Center for Child Health and Development, Tokyo, Japan
[4]Division of Otorhinolaryngology, National Center for Child Health and Development, Tokyo, Japan

Received 20 February 2008; Accepted 3 May 2008

How to cite this article: Iso M, Fukami M, Horikawa R, Azuma N, Kawashiro N, Ogata T. 2008. *SOX10* mutation in Waardenburg syndrome type II. Am J Med Genet Part A 146A:2162–2163.

To the Editor:

Waardenburg syndrome (WS) is a congenital developmental disorder characterized by sensorineural hearing loss and abnormal pigmentation of the eye, hair, and skin [Jones, 2006]. This condition is divided into four types [reviewed in Jones, 2006; Bondurand et al., 2007]. Type I WS (WS1) consists of dystopia canthorum and broad nasal root, and is almost exclusively caused by heterozygous mutations of *PAX3*. Type II WS (WS2) lacks the dystopia canthorum and results from heterozygous mutations of *MITF* (WS2A) in ~15% of patients and homozygous deletions of *SNAI2* (WS2D) in two patients. Type III WS (WS3) (Klein–Waardenburg syndrome), a severe form of WS1, is associated with upper limb defects, and is ascribed to heterozygous or homozygous mutations of *PAX3*. Type IV WS (WS4) (Shah–Waardenburg syndrome) is characterized by Hirschsprung disease, and is caused by heterozygous or homozygous mutations of *EDNRB* or its ligand *EDN3*, or by heterozygous mutations of *SOX10*.

Thus, the underlying causes remain to be clarified in most of the WS2 patients. While a WS2 locus is mapped to chromosome 1p (WS2B) [Lalwani et al., 1994] and chromosome 8q23 (WS2C) [Selicorni et al., 2002], a causative gene(s) has not been identified from these regions. In this regard, Bondurand et al. [2007] have recently identified *SOX10* deletions in patients with WS2, implying that *SOX10* abnormalities can cause WS2 (WS2E) as well as WS4. Here, we describe another case of WS2E caused by heterozygous *SOX10* mutation.

This Japanese girl was born to nonconsanguineous healthy parents at 41 weeks of gestation after an uncomplicated pregnancy and delivery. At birth, her length was 49.6 cm (+0.6 SD), and her weight 3.4 kg (+0.1 SD). She was found to have light blue eyes, and referred to us at 12 days of age. She manifested hypopigmented irides and a piece of white forelock, but lacked dystopia canthorum, broad nasal root, and Hirschsprung disease. Ophthalmologic examinations revealed bilateral ocular albinism with hypopigmented fundus and hypochromic iris. At 3.5 months of age, auditory brainstem response was performed because of poor responses to sounds, showing bilateral severe sensorineural deafness (hearing level, 90 dB bilaterally). Brain computed tomography showed no abnormal finding. On the basis of the above findings, she was diagnosed as having WS2.

After obtaining written informed consent, direct sequencing was performed for leukocyte genomic DNA of this patient, detecting no abnormality in the coding sequences of *PAX3*, *MITF*, and *SNAI2*. However, we identified a heterozygous *SOX10* frameshift mutation (c.506delC) on exon 4 that is predicted to result in a premature termination at the 284th amino acid (p.Pro169fsX284) (Fig. 1A). The primer sequences and the annealing temperature used were: exon 3, GTTGGACTCTTTGCGAGGAC and ATCCACCCGAAGCTAGAGG (58°C); exon 4, AGCCCCTCTGCTGTCCTCT and CACCCTCAGCTCTGTCATCA (60°C); and exon 5, CTAACCTGCTTCCCCCTTG and CAAGGAACAGGGCACACAG (58°C). This frameshift mutation located within the high mobility group (HMG) DNA-binding domain, and removed the C-terminal part of the HMG domain and the whole transactivation domain. This mutation is predicted to destroy an *NciI* restriction site, and

*Correspondence to: Tsutomu Ogata, M.D., Department of Endocrinology and Metabolism, National Research Institute for Child Health and Development, Tokyo 157-8535, Japan. E-mail: tomogata@nch.go.jp

Published online 14 July 2008 in Wiley InterScience (www.interscience.wiley.com)
DOI 10.1002/ajmg.a.32403

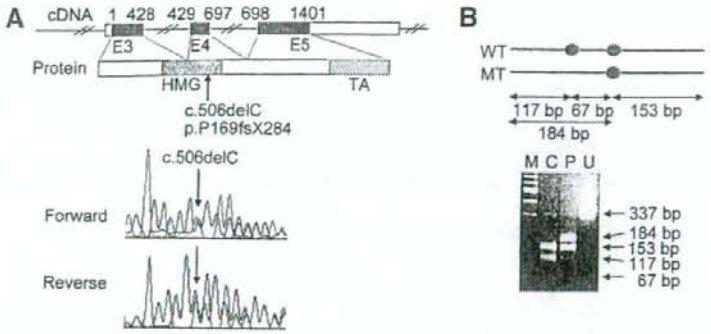

FIG. 1. Mutational analysis of *SOX10*. **A**: Direct sequencing of exon 4. Shown on the upper part is a schematic representation indicating the coding exons 3–5 (E3–E5) and the functional domains. For the *SOX10* cDNA, the black and white areas denote the coding regions and the untranslated regions, respectively, and the Arabic numbers indicate the cDNA sequence encoded by each exon. For the SOX10 protein, the gray and striped squares represent the high mobility group (HMG) DNA-binding domain and the transactivating (TA) domain. Electrochromatograms (forward and reverse) indicate a heterozygous c.506delC mutation on exon 4. **B**: Restriction enzyme analysis. The black circles represent *NciI* restriction sites. PCR products contain naturally occurring two *NciI* sites on the wild-type (WT) exon 4, and one of the two *NciI* sites is predicted to be destroyed on the mutant (MT) exon 4. After *NciI* digestion, WT sequence specific 117 and 67 bp bands only are found for a control subject (C), whereas WT specific 117 bp and 67 bp bands and a MT specific 184 bp band are shown for the patient (P). M: size marker; and U: undigested PCR product (337 bp).

this was confirmed by the *Nci*I digestion of the corresponding PCR products (Fig. 1B). While the parents postponed the decision to have the genetic testing, this mutation was absent in 100 control subjects.

The results provide further support for the notion that WS2 can be caused by heterozygous abnormalities of *SOX10* (WS2E). In this regard, a *SOX10* frameshift mutation (c.1076–1077delGA, p.Thr360fs X399) has been identified not only in a patient with a typical WS4 but also in the mother with an apparently WS2-compatible deafness and white forelock only phenotype [Pingault et al., 1998]. In addition, another *SOX10* missense mutation (p.Ser135Thr) has also been detected in a patient with "Yemenite deaf-blind hypopigmentation syndrome" mimicking WS2 [Bondurand et al., 1999]. These findings, together with *SOX10* deletions in patients with WS2 [Bondurand et al., 2007], imply that heterozygous *SOX10* abnormalities lead to not only WS4 but also to the WS2 phenotype. Such phenotypic variability would not be unexpected, because it is known that heterozygous mutations of developmental genes are usually associated with wide range of expressivity and penetrance [Fisher and Scambler, 1994]. In addition, the position of the frameshift mutation on exon 4 may also be relevant to the lack of associated features, because *SOX10* mutations residing on the last exon frequently lead to more severe phenotypes such as chronic intestinal pseudo-obstruction and/or neurological features, probably due to escape from the nonsense mediated mRNA decay [Pingault et al., 2000, 2002; Inoue et al., 2004].

REFERENCES

Bondurand N, Kuhlbrodt K, Pingault V, Enderich J, Sajus M, Tommerup N, Warburg M, Hennekam RC, Read AP, Wegner M, Goossens M. 1999. A molecular analysis of the yemenite deaf-blind hypopigmentation syndrome: SOX10 dysfunction causes different neurocristopathies. Hum Mol Genet 8:1785–1789.

Bondurand N, Dastot-Le Moal F, Stanchina L, Collot N, Baral V, Marlin S, Attie-Bitach T, Giurgea I, Skopinski L, Reardon W, Toutain A, Sarda P, Echaieb A, Lackmy-Port-Lis M, Touraine R, Amiel J, Goossens M, Pingault V. 2007. Deletions at the SOX10 gene locus cause Waardenburg syndrome types 2 and 4. Am J Hum Genet 8:1169–1185.

Fisher E, Scambler P. 1994. Human haploinsufficiency—One for sorrow, two for joy. Nat Genet 7:5–7.

Inoue K, Khajavi M, Ohyama T, Hirabayashi S, Wilson J, Reggin JD, Mancias P, Butler IJ, Wilkinson MF, Wegner M, Lupski JR. 2004. Molecular mechanism for distinct neurological phenotypes conveyed by allelic truncating mutations. Nat Genet 36:361–369.

Jones KL. 2006. Waardenburg syndrome, types I and II. In: Jones KL, editor. Smith's recognizable patterns of human malformation. Philadelphia: Elseview Saunders. p 278–279.

Lalwani AK, Baldwin CT, Morell R, Friedman TB, San Agustin TB, Milunsky A, Adair R, Asher JH, Wilcox ER, Farrer LA. 1994. A locus for Waardenburg syndrome type II maps to chromosome 1p13.3–2.1. Am J Hum Genet 55:A14.

Pingault V, Bondurand N, Kuhlbrodt K, Goerich DE, Préhu MO, Puliti A, Herbarth B, Hermans-Borgmeyer I, Legius E, Matthijs G, Amiel J, Lyonnet S, Ceccherini I, Romeo G, Smith JC, Read AP, Wegner M, Goossens M. 1998. SOX10 mutations in patients with Waardenburg-Hirschsprung disease. Nat Genet 18:171–173.

Pingault V, Guiochon-Mantel A, Bondurand N, Faure C, Lacroix C, Lyonnet S, Goossens M, Landrieu P. 2000. Peripheral neuropathy with hypomyelination, chronic intestinal pseudo-obstruction and deafness: A developmental "neural crest syndrome" related to a SOX10 mutation. Ann Neurol 48:671–676.

Pingault V, Girard M, Bondurand N, Dorkins H, Van Maldergem L, Mowat D, Shimotake T, Verma I, Baumann C, Goossens M. 2002. SOX10 mutations in chronic intestinal pseudo-obstruction suggest a complex physiopathological mechanism. Hum Genet 111:198–206.

Selicorni A, Guerneri S, Ratti A, Pizzuti A. 2002. Cytogenetic mapping of a novel locus for type II Waardenburg syndrome. Hum Genet 110:64–67.

黄斑を形成する遺伝子システムと再生医療への応用

Gene mechanism that relates to formation of the fovea and its contribution to reproducing medicine

東　範行
Noriyuki Azuma
国立成育医療センター眼科

◎黄斑は中心視力を得るための高度な網膜構造である．Pax6 はすべての動物における眼形成の master control 遺伝子であるが，ヒトの黄斑低形成で Pax6 遺伝子の変異が発見されたことから，黄斑の形成に関与していると思われる．Pax6 は選択的スプライスのエクソン 5a を含むアイソフォーム Pax6(+5a)と含まない Pax6(−5a)があり，異なる転写因子の働きをもつが，黄斑の形成には Pax6(+5a)がかかわっていることが示唆された．このような黄斑の形成にかかわる遺伝子システムを応用すれば，網膜の再生において高度な視覚を獲得できることが期待される．

Key word：黄斑，形態形成遺伝子，Pax6，選択的スプライス

黄斑は網膜において高度な視覚である中心視力をつかさどるために細胞が密に集中する特殊な部位である．この形成機構には何らかの遺伝子が働いているはずであるが，これまでほとんど検討されていなかった．先天性の黄斑低形成において眼の形成遺伝子 Pax6 の変異がみつかったことが発端になって，この遺伝子の働きが *in vitro*，*in vivo* で検討され，網膜の高度構造をつくるシステムが明らかになりつつある．

眼形成のmaster control遺伝子Pax6

Pax 遺伝子群は paired box と homeobox を共通モチーフとしてもつ遺伝子ファミリーで，422 のアミノ酸をコードする．Pax 蛋白では paired box から翻訳される paired domain がおもに標的遺伝子に結合する(図 1)．この遺伝子群は最初にショウジョウバエで発見され，脊椎動物では 9 種みつかっており，Pax6 はその 6 番目にあたる．ヒトの Pax6 遺伝子は最初に先天無虹彩の原因遺伝子として染色体 11p13 領域の欠失部位から positional cloning によって発見された[1]．

その後，この遺伝子がマウスやラットで変異があると小眼球を起こす small eye(Sey)や，ショウジョウバエで複眼が形成されない eyeless と相同であることが判明した．さらに，ショウジョウバエ初期胚のさまざまな部位にこの遺伝子を導入すると(target expression)，触覚や翅，肢などに異所性に複眼が発生したことから，眼の器官全体をつくる強力な形態形成遺伝子であることが明らかになった[2]．器官の形態形成には全体的に支配する master control 遺伝子があると予測されていたが，下等動物とはいえ，眼というもっとも複雑な器官でその遺伝子がいきなりみつかったのである(図 2)．

その後，さまざまな動物で Pax6 遺伝子がみつかり，脊椎動物，軟体動物の眼や昆虫の複眼だけでなく，プラナリアの原始眼や線虫の光感受性細胞にも存在しており，塩基配列が高度に保存されていたことから，眼の起源に関する考えに大きな転換をもたらした．動物には，種によって複眼，鏡眼，カメラ眼などさまざまな形態の眼があり，従来は 40〜60 系統が別々に発生した(収斂進化)と考えられていた．しかし，Pax6 がすべての動物

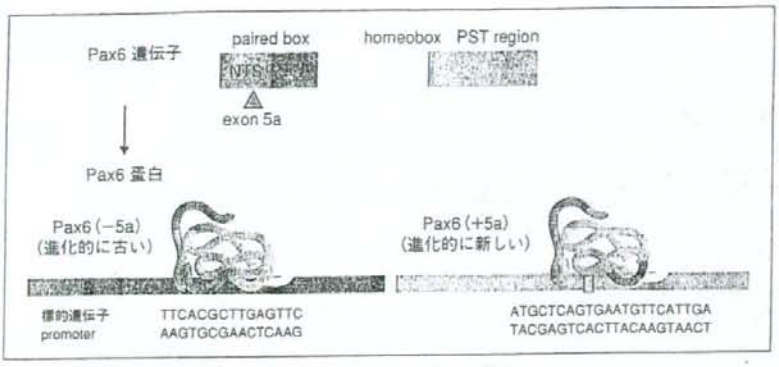

図 1　Pax6遺伝子と蛋白の構造

主要構造として，paired domain(標的 DNA に接触する部位，ここに相当する遺伝子配列を paired box という)，homeodomain(標的 DNA に接触するとともに形態形成遺伝子に特徴的な配列，遺伝子では homeobox)，末尾にプロリン，セリン，スレオニンを多く含む activating domain をもつ．エクソン 5 とエクソン 6 の間に 14 のアミノ酸をコードする選択的スプライスのエクソン 5a があり，2 種類のアイソフォームがつくられる．Paired domain はさらに N-terminal subdomain(NTS)と C-treminal subdomain(CTS)の 2 つに分かれ，標的 DNA が異なる．エクソン 5a による 14 アミノ酸が入れば CTS が，入らなければ NTS が働く．

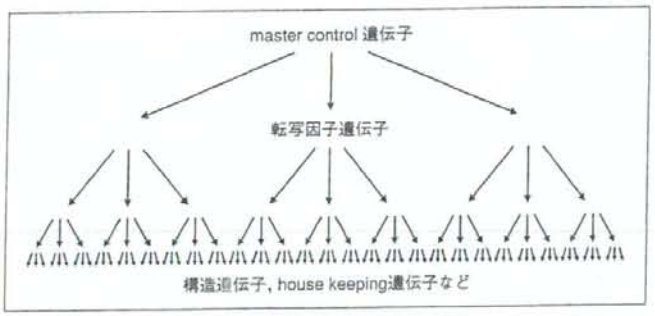

図 2　転写因子遺伝子カスケード

発生において組織ごとに上流遺伝子が下流を支配し，その頂点に器官形成全体を統合する master control 遺伝子が存在する．

の眼に存在することから，眼が原始の祖先動物で光を感じる細胞としてただ一度だけ出現し，進化とともに多彩な形態をとるようになったという単一起源説が支持されるようになった[2]．

Pax6遺伝子の変異によって起こるヒト眼形成異常

In situ hybridization や免疫染色によって Pax6 の発現を検討すると，発生初期は中枢神経や眼原基，中枢神経では前脳，後脳，神経管脳室復側，下垂体，嗅脳，眼ではまず視溝，ついで眼胞，表面外胚葉と水晶体板，網膜，角膜の順で，眼球ほぼ全体を網羅している(図 3)[3]．以上から，この遺伝子に変異が起こればきわめて多くの先天異常を起こすと推察された．

先天無虹彩では多くの変異が見出されてきたが，そのほかにも Peters 奇形のような前眼部形成不全，角膜ジストロフィー，瞳孔形成異常，先天白内障，黄斑低形成，視神経形成不全で変異がみつかり(図 4)[4-6]，Pax6 がヒトでも前眼部から眼底まで広い範囲で眼の形成を担っていることが分子遺伝学からも証明された．太古に光を感じる細胞

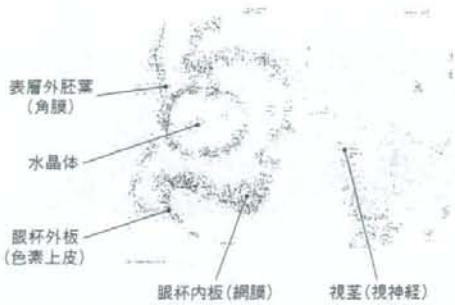

図 3 Pax6のモノクローナル抗体による発生ヒト眼(胎齢5週)の免疫染色[3]
発生初期では眼球のほぼ全体が染まる.

から出発した遺伝子が進化とともに眼形態形成の中心にいつづけて,角膜,虹彩,水晶体,網膜をつくるようになり,ついには視覚進化の頂点である黄斑を形成するに至ったことになる.

これまでにみつかったPax6の変異型と表現型には,遺伝子の変異が重篤なほど表現型も重症であるという法則がある.これはPax6に,①一対の対立遺伝子の両方が揃っていないと正常に機能しない(haploinsufficiency),②遺伝子障害の程度と表現型が相関する(dose dependent),という特徴があるためである.変異形式がストップコドン,フレームシフト,スプライシングエラーといったナンセンス変異では無虹彩のような眼球全体の形成不全を起こし,1アミノ酸が置換した軽度なミスセンス変異では角膜,水晶体,網膜などで限局した形成不全を起こす.黄斑のみの形成不全がある孤立性黄斑低形成でみつかった変異はいずれもミスセンス変異である[4-6].

Pax6の選択的スプライスの働きと黄斑低形成の遺伝子変異

Pax6遺伝子には,エクソン5とエクソン6の間に,14のアミノ酸をコードする選択的スプライスのエクソン5aが存在する.そして,これが読まれるか読まれないかによって,Pax6蛋白は14アミノ酸が入るもの〔Pax6(+5a)〕と入らないもの〔Pax6(−5a)〕,2種類のアイソフォームがつくられる[5].Pax6蛋白では,転写因子として標的DNAに接着する部位のpaired domainがあるが,14アミノ酸はこのなかに存在する.paired domainはさらにN-terminal subdomainとC-terminal subdomainの2つに分かれ,異なるタイプのbinding consensusをもつ標的DNAを支配する.しかも生化学的検討によれば両subdomainはたがいの働きを抑制しあっている.そして,エクソン5aによる14アミノ酸が入ればC-terminalが,入らなければN-terminalが働くので,エクソン5aはmolecular switchの働きをもっている(図1)[5].Pax6の進化からみると,N-terminal subdomainは原始的動物にある基本的なもので,標的DNAもいくつか判明している.一方,エクソン5aは無脊椎動物では存在せず,脊椎動物に至って出現したので,C-terminal subdomainが働きはじめたのは進化的に比較的新しい.しかも,その機能はまったく不明で,標的遺伝子もみつかっていない.

これまでに発見された孤立性黄斑低形成のPax6ミスセンス変異はことごとくC-terminal subdomainあるいはエクソン5aのなかに存在する[4,5].したがって,黄斑の形成にはこのC-terminal subdomainが関与していると推測された.

黄斑発生領域におけるPax6アイソフォームの発現

発生期の動物で時期別,眼組織別にmRNAを採取してcDNAを作成し,Pax6の2つのアイソフォームをRT-PCRで検討すると,Pax6(−5a)は発生期全般にわたって広範な組織に発現する.しかし,Pax6(+5a)は発生期後半に後方網膜に強く発現することが示された.さらに免疫染色では,Pax6(−5a)に対する抗体では網膜は後方から前方まで均一に染まるのに対して,エクソン5aがコードする14アミノ酸に対する抗体では黄斑領域を中心とする後極のみに染色がみられ,Pax6(+5a)は黄斑領域に限局して発現することが判明した(図5)[7].

Pax6アイソフォームの網膜形成・分化に関する機能

Pax6が黄斑形成に関与するならば,発生期の網膜にPax6を過剰に導入すると網膜の形成が進むはずである.しかし,過去の研究報告は逆の結果

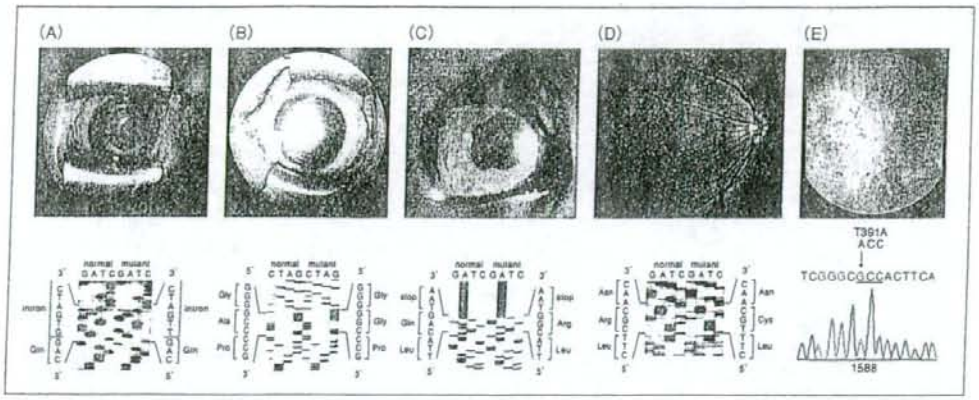

図 4　Pax6の変異がみつかった眼先天異常[4~6]
A：無虹彩，B：前眼部形成不全，C：瞳孔形成異常，D：黄斑低形成，E：視神経低形成．

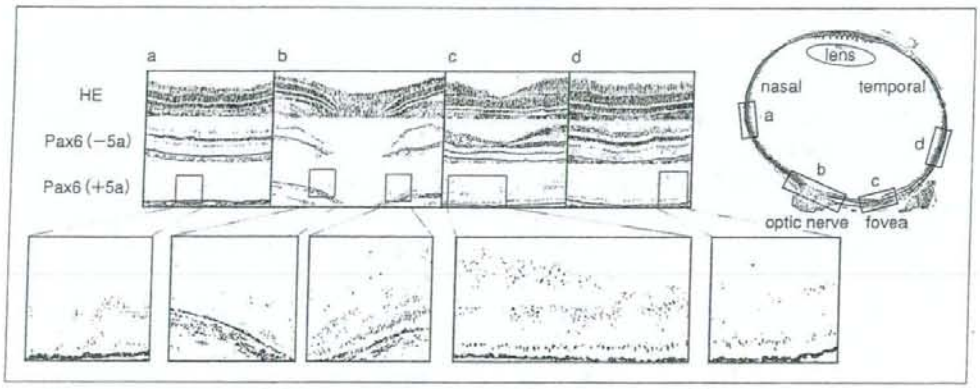

図 5　Pax6アイソフォームの発生期網膜における発現[7]
出生直後のマーモセット Pax6(−5a)に対する抗体では，網膜は後方から周辺部まで均一に染まるのに対して，エクソン 5a がコードする 14 アミノ酸に対する抗体では黄斑領域を中心とする後極のみに染色がみられる．Pax6(+5a)は黄斑領域に限局して発現することが示唆される．

を示していた．Pax6 の変異をもつマウスは小眼球になるが，一方で，Pax6 を過剰に導入したトランスジェニックマウスをつくっても小眼球が生ずる[8]．ここから Pax6 の発現量は少なくても多過ぎても正常に機能しないという考えが定着した．しかし，トランスジェニックマウスでは，導入した Pax6 が眼球だけでなく，中枢や視神経など多くの組織に発現する．小眼球は発生のわずかな均衡がくずれれば容易に起こるので，多くの組織に Pax6 が異常量発現すれば，組織間相互作用が障害され，結果として小眼球になることも考えられる．網膜への Pax6 の影響を知るためには網膜だけに遺伝子を導入しなければならない．そこでニワトリの発生期網膜に electroporation で Pax6 を直接導入した．Electroporation で導入した遺伝子は細胞質内で短期間発現するので，発生のような一時期に働く遺伝子の機能を観察する点では都合がよい．

発生初期(stage 12~16)の網膜に，エクソン 5a を含まない Pax6 のアイソフォーム Pax6(−5a)を導入すると網膜が厚くなり，神経節細胞が増加し(図 6-B)，神経線維が硝子体腔に向かって増加した(図 6-C)．導入直後では神経芽細胞の分裂が亢

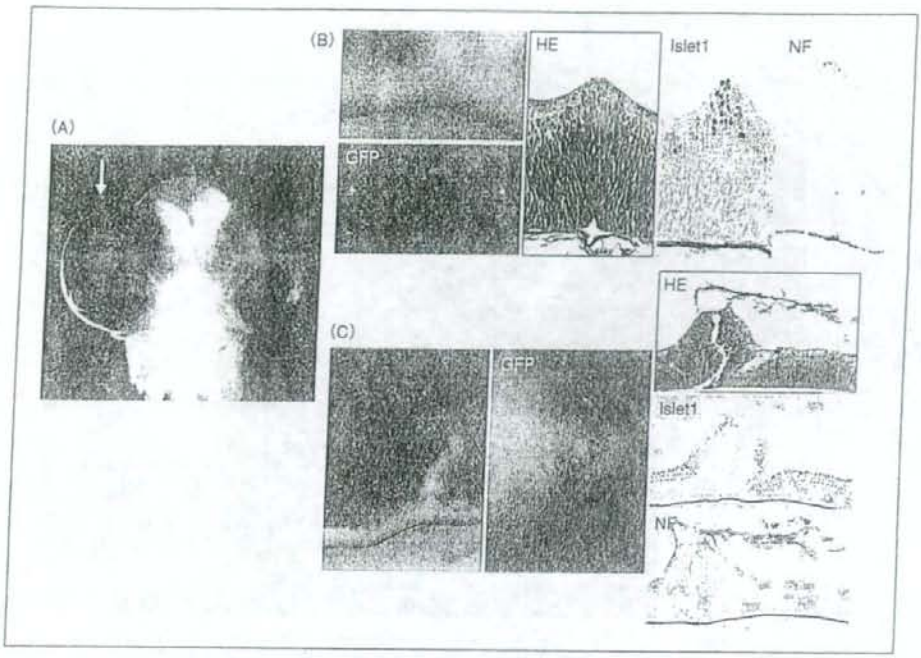

図 6　鶏胚へのPax6(−5a)導入による網膜の発育亢進[17]

2 日胚に導入，8 日胚の所見．

A：Pax6(−5a)を入れた右眼が大きくなる(矢印)．B：網膜が厚くなり，GFP で遺伝子の導入が確認され，組織所見では神経節細胞が増加している．C：網膜から硝子体腔へ線維構造が立ち上がり，組織所見では神経線維である．

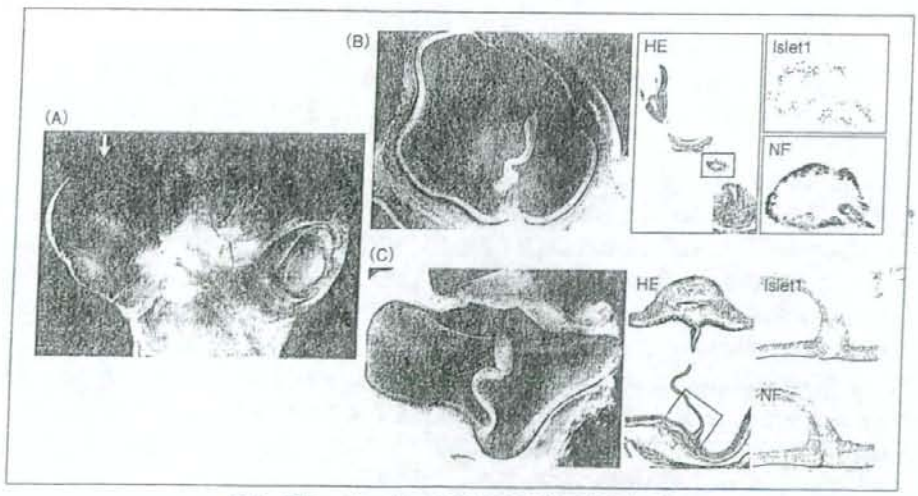

図 7　鶏胚へのPax6(＋5a)導入による網膜の発育亢進[17]

2 日胚に導入，10 日胚の所見．

A：Pax6(＋5a)を入れた右眼が極度に大きくなる(矢印)．B：網膜から茎状構造が立ち上がり，組織所見では管状の網膜で層構造はほぼ保たれている．C：網膜が水平に過剰発育して折りたたまれている．

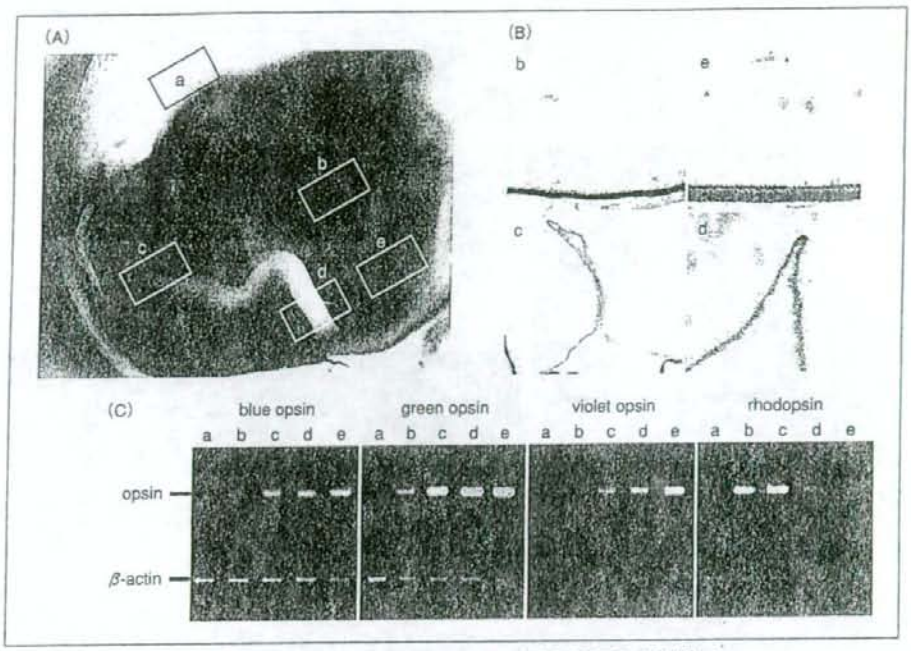

図 8　鶏胚へのPax6(+5a)導入による異所性錐体細胞の形成[7]
2 日胚に導入，19 日胚の所見．A：網膜が過剰に発育した嚢を形成．この嚢内では，周辺部(c)に本来は少ないオプシンをもつ錐体細胞が形成されている．B：免疫染色，C：RT-PCR．

進しており，Pax6 は網膜の成長を担っていると考えられた[7]．

つぎに，エクソン 5a を含む Pax6(+5a)を導入すると網膜から硝子体腔へ茎状構造が立ちあがった．これはすべて網膜であり，神経細胞と神経線維で構成されていた．茎状に伸びた組織では網膜が管状になっており，しかも視細胞から神経節細胞に至る層構造がほぼ形成されていた(図 7-B)．また，網膜が硝子体腔へ折りたたまれる所見もみられた(図 7-C)．網膜が水平方向へ過剰に発育し，抵抗の少ない硝子体腔へ伸展したと考えられる．

したがって，網膜を成長させる働きは Pax6(−5a)より Pax6(+5a)のほうがはるかに強いことが明らかになった．さらに，錐体視細胞が少なく杆体細胞がおもに存在する網膜周辺部に Pax6(+5a)を導入すると，異所性に錐体細胞の形成が観察された(図 8)[7]．この Pax6(+5a)による網膜の発育と錐体細胞の分化が硝子体腔へ突出せず網膜内の 1 カ所に集中すれば，黄斑になるのかもしれない．

Pax6 を入れた領域の眼球は拡大し，角膜と水晶体が対側へ偏位した．この作用は Pax6(−5a)より Pax6(+5a)のほうが強かった(図 6-A，図 7-A)[7]．眼球は発生初期には頭の横にあり，鼻側と耳側が同じ大きさであるが，発生が進むと眼球の位置が頭の横から顔の前へ向くとともに耳側が大きくなる．網膜の成長が進むと眼球が成長し，一方，網膜の形成不全では小眼球になることから，眼球の大きさには網膜の成長が関わっている．眼球の耳側が鼻側に比べて大きいのは Pax6(+5a)が耳側後極で強く発現して網膜の発育を進めるためであると考えられる．Pax6 にこのエクソン 5a が現れたのは脊椎動物になってからであるが，魚類で網膜の構造は急速に複雑化し，黄斑が生まれたのは，このエクソン 5a の追加が関与したことも示唆される．

Pax6などの眼形成遺伝子を用いた網膜の再生

Pax6/eyeless を異所導入すると昆虫ではほぼ完

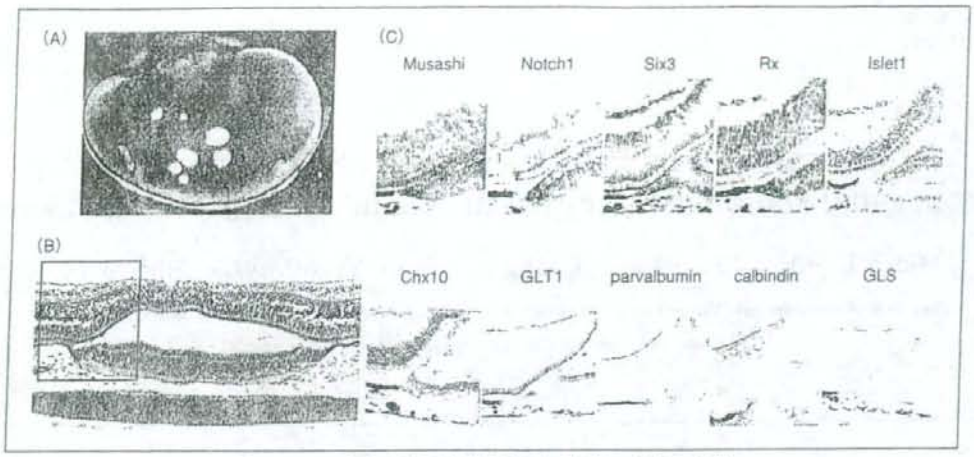

図 9　Pax6の導入による網膜色素上皮から網膜への分化転換[17]
3 日胚に導入，14 日胚の所見．遺伝子が導入された色素上皮は斑状に(A)，網膜へ分化転換している(B)．この異所網膜は *in situ* hybridization や免疫染色で網膜固有の遺伝子・蛋白発現がみられ(C)，ほぼ完全な層構造をもつが，層の方向は眼杯が折りたたまる向きに応じて本来の網膜と背合わせになっている．

全な複眼が形成される[2]．Pax6/eyeless 下流の eyes absent, sine oculis/Six, dachshund, Rx, teashirt の導入では小さい複眼が形成されるが[9-12]，哺乳類では，Pax を導入してもアフリカツメガエルの幼生で不完全な構造の異所眼が形成されるにすぎない[13]．また，Six6，Rx を発生期の脳や網膜色素上皮に導入すると，不完全ながら網膜組織が形成されるが[14-16]，Pax6 を導入するとかなり完全な層構造をもつ網膜を形成することができる(図 9)[17]．この網膜形成における Pax6(−5a)と Pax6(+5a)の働きの違いは現在検討中であるが，過去の研究からみて Pax6(+5a)のほうがより高度な網膜を形成できる可能性がある[7]．

近年，網膜色素変性症モデル動物や患者で，障害された黄斑部網膜下に胎児網膜を移植して視力が改善したことが報告された[18,19]．未熟な胎児網膜がレシピエント網膜内で分化し，シナプスを形成すると思われる．網膜色素変性症では視細胞以外の網膜構造はある程度温存されており，胎児網膜由来の視細胞のシナプスがつながったと推測される．自己の虹彩や色素上皮に網膜の形態形成遺伝子を導入あるいは発現誘導して網膜を再生できれば，やや不完全な構造であっても，このような網膜移植に利用できることが期待される．

おわりに

網膜の重症疾患で悩まされている患者や医師にとって，網膜を再生させて失われた視覚を復元させる医療は大きな夢である．しかし，構造が複雑な網膜をシナプスごと再構築することが難しく，中枢への神経投射を的確に復元しないかぎり有用な視力が得られない．できても，せいぜい光覚や手動弁の視力あるいは視野をすこし広げる程度と考えられていた．しかし，近年の再生医学研究によって視覚の復元への道はすこしずつ着実に進歩している．黄斑を形成する遺伝子システムを解明して再生医療に利用すれば，高度な視覚構造が復元できると期待される．

文献

1) Ton, C. T. T. et al. : *Cell*, 67 : 1059-1074, 1991.
2) Callaerts, P. et al. : *Annual. Rev. Neurosci.*, 20 : 483-532, 1997.
3) Nishina, S. et al. : *Br. J. Ophthalmol.*, 83 : 723-727, 1999.
4) Azuma, N. et al. : *Nat. Genet.*, 13 : 141-142, 1996.
5) Azuma, N. et al. : *Am. J. Hum. Genet.*, 65 : 656-663, 1999.
6) Azuma, N. et al. : *Am. J. Hum. Genet.*, 72 : 1565-1570, 2003.
7) Azuma, N. et al. : *Hum. Mol. Genet.*, 14 : 735-745, 2005.
8) Schedl, A. et al. : *Cell*, 86 : 71-82, 1996.

Available online at www.sciencedirect.com

ScienceDirect

Vision Research 48 (2008) 273–280

Vision Research

www.elsevier.com/locate/visres

Comparison of focal macular cone ERGs in complete-type congenital stationary night blindness and APB-treated monkeys ☆

Mineo Kondo *, Shinji Ueno, Chang-Hua Piao, Yozo Miyake, Hiroko Terasaki

Department of Ophthalmology, Nagoya University Graduate School of Medicine, 65 Tsuruma-cho, Showa-ku, Nagoya 466-8550, Japan

Received 1 August 2007; received in revised form 9 November 2007

Abstract

Focal macular cone electroretinograms (ERGs) and multifocal ERGs were recorded to study the macular function in patients with the complete-type of congenital stationary night blindness (cCSNB). The waveforms of the focal macular cone ERGs and the on- and off-responses of the multifocal ERGs in the cCSNB patients were similar to those recorded from monkey retinas treated with L-2 amino-4-phosphonobutyric acid (APB), suggesting that patients with cCSNB have a complete defect of the on-pathway even in the central retina. The results also demonstrated that there was a paradoxical positive response in the central retina of cCSNB patients, as compared to the negative full-field ERGs in the same subjects.

Keywords: Electroretinogram (ERG); Focal macular cone ERG; Congenital stationary night blindness (CSNB); Complete-type; APB (L-2 amino-4-phosphonobutyric acid)

1. Introduction

The complete-type of congenital stationary night blindness (cCSNB) is a non-progressive retinal disease characterized by congenital night blindness with a moderate decrease of the visual acuity and myopia (Miyake, Horiguchi, Suzuki, Kondo, & Tanikawa, 1997; Miyake, Yagasaki, Horiguchi, Kawase, & Kanda, 1986). The inheritance pattern of cCSNB is usually X-linked or autosomal recessive. It was recently reported that most X-linked cCSNB resulted from mutations in the *NYX* gene (Bech-Hansen et al., 2000; Pusch et al., 2000), and some cases of autosomal recessive cCSNB resulted from mutations in the *MGR6* gene (Dryja et al., 2005).

cCSNB patients have very characteristic electroretinograms (ERGs). When elicited by a bright stimulus after dark-adaptation, the ERGs are the negative-type with an a-wave of normal amplitude and a b-wave that is smaller than the a-wave. When a long-duration photopic stimulus is used, the b-waves of the ERGs of cCSNB patients are severely reduced while the off-response d-wave is well-preserved (Houchin, Purple, & Wirtschafter, 1991; Miyake, Yagasaki, Horiguchi, & Kawase, 1987; Young, 1991). These ERG waveforms are very similar to those in the monkey photopic ERGs after an intravitreal injection of 2-amino-4-phosphonobutyric acid (APB), which blocks neurotransmission from photoreceptors to the on-bipolar cells (Evers & Gouras, 1986; Knapp & Schiller, 1984; Sieving, Murayama, & Naarendorp, 1994). These results demonstrated that the defect in the neural pathway of cCSNB patients lies in the signal transmission from the photoreceptors to the depolarizing on-bipolar cells (DBCs) in both the rod and cone pathways. Recent ERG analysis using sinusoidal and ramping on/off flicker stimuli also indicated that the deficit in eyes with cCSNB is localized to the DBC pathway with no apparent involvement of the hyperpolarizing off-bipolar cells (HBCs) (Khan et al., 2005).

☆ *Grant support:* Grant-in Aid 14770952 (M.K.), and 14370557 (H.T.) from the Ministry of Education, Science, Sports and Culture, Japan.
* Corresponding author. Fax: +81 52 744 2278.
E-mail address: kondomi@med.nagoya-u.ac.jp (M. Kondo).

0042-6989/$ - see front matter © 2007 Elsevier Ltd. All rights reserved.
doi:10.1016/j.visres.2007.11.010

Although there are many electrophysiological studies on the full-field ERG in patients with cCSNB, there are very few studies on the macular function of eyes with cCSNB using either the multifocal or focal macular cone ERG techniques (Kondo et al., 2001; Leifert, Todorova, Prunte, & Palmowski-Wolfe, 2005). During our extensive studies of the complete and incomplete type of CSNB, we have been gaining the impression that the cone on-pathway may be functioning relatively well only in the central retina in cCSNB because these patients have relatively good visual function in the central field (Miyake et al., 1997; Terasaki et al., 1999).

The purpose of this study was to investigate the macular function of patients with cCSNB in more detail using focal macular cone ERGs and multifocal ERGs. To accomplish this, we separated the on- and off-responses of the photopic ERGs using long-duration photopic stimuli in the macular area of patients with cCSNB, and then compared the obtained waveforms with those recorded from monkey retinas in which the on-pathway was completely blocked pharmacologically by an intravitreal injection of L-2 amino-4-phosphonobutyric acid (APB).

2. Materials and methods

2.1. Patients with complete-type CSNB

From the patients with cCSNB examined in our clinic (Department of Ophthalmology, Nagoya University Hospital), we selected three patients who agreed to participate and were cooperative with the electrophysiological examinations (Table 1). All patients had poor night vision from birth and had no fundus abnormalities except for myopic changes. Their corrected visual acuities were 0.4, 0.4, and 0.6, and the rod branch of the dark-adaptation curve was missing as determined by psychophysical dark adaptometry. The full-field ERG rod responses were undetectable, and the rod and cone mixed maximal ERG had a negative-shape with no detectable oscillatory potentials.

An informed consent was obtained from the three patients after a full explanation of the procedures. All studies were conducted in accordance with the principles embodied in the Declaration of Helsinki.

2.2. Animals

Four rhesus (*Macaca mulata*) monkeys were studied under protocols approved by Nagoya University School of Medicine. All experiments were conducted in accordance with NIH guidelines on animal use and with the ARVO statement on the Use of Animals in Ophthalmic and Vision Research. The animals were anesthetized with intramuscular injection of ketamine hydrochloride (7 mg/kg, 5–10 mg/kg/h maintenance dose) and xylazine (0.6 mg/kg). The respiration and heart rate were monitored, and hydration was maintained by a slow, continuous infusion of lactated Ringer solution. The cornea was anesthetized by topical 1% tetracaine, and the pupil was dilated with topical 0.5% tropicamide, 0.5% phenylephrine HCL, and 1% atropine.

2.3. Drug application to animals

The drugs were injected into the vitreous with a 30-gauge needle inserted through the pars plana approximately 3 mm posterior to the limbus. The drugs (Sigma Chemical Co., St. Louis, MO) were dissolved in sterile saline and injected in amounts of 0.05–0.07 ml. The intravitreal concentration was 1–2 mM for L-2 amino-4-phosphonobutyric acid (APB) and 5 mM for *cis*-2, 3 piperidine dicarboxylic acid (PDA). Recordings were begun about 60–90 min after the drug injections, and studies were completed within 5 h. Although the drug effects are mostly reversible after a recovery period of several weeks, the results that are presented were recorded from the eyes not previously treated.

2.4. Focal macular cone ERG

Focal macular cone ERGs were elicited by stimulating the macula with small stimulus spots (Miyake, 1988b; Miyake, Shiroyama, Ota, & Horiguchi, 1988a). The position of the spot on the fundus was monitored during the recording with a modified infrared fundus camera. The Burian-Allen bipolar contact lens electrode (Hansen Ophthalmic Development Laboratories, Iowa City, IA) which was used to record the focal macular cone ERGs, allowed a clear view of the fundus on the television monitor. The luminances of the stimulus and the background were 30.0 cd/m^2 and 3.0 cd/m^2, respectively. A 5-Hz rectangular stimulus (100 ms-on and 100 ms-off) was used with a stimulus spot of 15 degrees in diameter. A total of 512 responses were averaged by a signal processor, and the time constant was 0.03 s with a 300-Hz high-cut filter. The ERG responses produced by this method are generated by the cone system, and the responses elicited by the spot stimuli are considered to be local responses (Miyake, 1988b; Miyake et al., 1988a).

2.5. Recording multifocal on- and off-responses

Our method for recording on- and off-responses of the multifocal ERGs has been described in detail (Kondo & Miyake, 2000; Kondo, Miyake, Horiguchi, Suzuki, & Tanikawa, 1998). In brief, multifocal ERGs were obtained with the VERIS system (EDI, San Mateo, CA). The stimulus array consisted of 61 hexagonal elements that were displayed on a CRT monitor (GDM, Sony, Tokyo, Japan) and driven at 75 frames/s. At a viewing distance of 27 cm, the subtense of the visual field was approximately 50°.

To obtain on- and off-responses with the VERIS system, we used consecutive white TV frames. Each hexagon was modulated between two stimulus patterns according to a binary m-sequence: eight consecutive white frames followed by eight consecutive dark frames (pattern A) or 16 consecutive dark frames (pattern B). In this stimulus setting, a stimulus is not continuously bright during its bright phase because the focal flash decays within a few milliseconds. However, there is evidence that a high-frequency train of flashes can roughly simulate the effects produced by a long-duration stimulus and thus can produce a corneal positive off-response (Saeki & Gouras, 1996; Young, 1991).

Based on our preliminary study, the following stimulus parameters were found to be suitable for eliciting maximal on- and off-responses from each local retinal area: stimulus intensity of 120 cd/m^2 with a duration of 8 frames (106 ms) on a 20 cd/m^2 background illumination. The m-sequence stimulation rate was, therefore, 4.7/s and the base interval was 213.3 ms (Kondo & Miyake, 2000; Kondo et al., 1998).

Table 1
Clinical characteristics of three patients with complete type CSNB

Case	Age	Sex	Inheritance pattern	Refractive error (*D*)	Visual acuity
Case 1	54	M	Autosomal recessive	−4.0	0.4
Case 2	20	M	X-linked	−9.5	0.4
Case 3	15	F	Autosomal recessive	−6.0	0.6

The signals were amplified by 100 K and filtered between 3 and 300 Hz (Grass, Quincy, MA). The data sampling rate was 1200 Hz. To reduce the artifacts due to eye movements, an "artifact rejection" algorithm (VERIS software, EDI) was used once (Marmor et al., 2003). The length of the m-sequence used was 2^{11}–1. Thus, the total recording took 7.3 min, and it was divided into 16 segments.

For recording multifocal ERGs from monkeys, a modified ophthalmoloscopic technique was used to locate the projection of the fovea on the center of the stimulus pattern (Rangaswamy, Hood, & Frishman, 2003). This modified ophthalmoscope was kindly provided by Dr. L. Frishman (University of Houston). The position of the fovea was checked frequently before and after the multifocal ERG recordings.

2.6. Recording full-field ERGs

Full-field ERGs were recorded with long-duration stimuli (166 ms or 100 ms) using a densely-packed array of 102 green LEDs (525 nm peak wavelength; 50 nm at half-amplitude). The array was positioned at the top of the Ganzfeld dome and covered by a diffuser (Ueno et al., 2006). The LEDs were controlled by a digital function generator (WF1945, NF Corporation, Tokyo, Japan). The stimulus intensity and background illumination measured in the dome was 120 cd/m^2 and 40 cd/m^2, respectively. In the last experiment, the stimulus intensity and background illumination was set at 30 cd/m^2 and 3 cd/m^2, respectively, in order to compare the waveforms of full-field ERG and focal macular cone ERG at the same stimulus and background condition.

After 10 min of light adaptation, ERGs were recorded with a Burian-Allen bipolar contact lens electrode (Hansen Ophthalmic Development Labs, Iowa City, IA). A ground electrode was attached to the ipsilateral ear. Responses were amplified by 10 K and the bandpass was set to 0.3–1000 Hz. The data were digitized at 4.3 kHz. Twenty responses were averaged (Power Lab, AD Instruments, Castle Hill, Australia).

3. Results

3.1. Focal macular cone ERGs in cCSNB

Representative focal macular cone ERGs recorded from a myopic control (38-year-old man; refractive error, −5.50 D) and the three patients with cCSNB are shown in the left panel of Fig. 1. The waveforms from the three patients are clearly different from those of the myopic control: the amplitudes of the a-waves are normal, but the amplitudes of the following positive wave are smaller than the b-wave of the myopic control (see also Table 2). These changes resulted in a reduced b-wave to a-wave (b/a) ratio. In addition, the implicit times of the a- and b-waves in

Table 2
Amplitudes and implicit times of focal macular ERGs (FMERGs) from three patients with complete type CSNB and 15 patients with myopic controls

	Amplitude (μV)			Implicit times (ms)	
	a-wave	b-wave	b/a ratio	a-wave	b-wave
Case 1	2.4	2.4	1.0	21.4	47.2
Case 2	1.9	2.9	1.56	28.0	46.8
Case 3	2.4	3.1	1.29	28.0	59.5
Myopic controls ($n = 15$)	2.0 ± 0.5	5.1 ± 0.9	2.51 ± 0.44	19.6 ± 1.7	40.9 ± 3.0

Data in myopic controls are expressed as the mean ± SD.

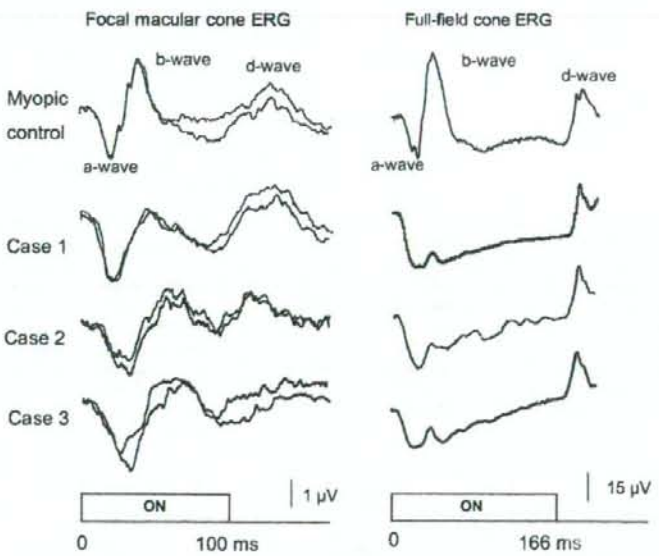

Fig. 1. Focal macular cone ERGs (left panel) and full-field ERGs (right panel) elicited by long duration stimuli recorded from a myopic control and three patients with complete-type congenital stational night blindness (cCSNB). Note that the amplitude ratios of the positive wave to the a-wave was <1.0 for the full-field ERG, but >1.0 for focal macular cone ERGs in the cCSNB patients.

cCSNB patients were prolonged (Table 2). The d-waves seen at the offset of the stimulus was not so prominent for both myopic controls and patients.

The full-field, photopic ERGs elicited by a long-duration stimulus (166 ms) from the same subjects are shown in the right panel of Fig. 1. In all three cCSNB patients, the b/a amplitude ratio was clearly <1.0 resulting in a "negative" ERG waveform.

3.2. Focal macular cone ERGs in monkey retina after APB

It is known that the on-response b-wave of the photopic long-flash ERG originates mainly from the neural activity of the cone depolarizing bipolar cells (DBCs) (Knapp & Schiller, 1984; Sieving et al., 1994). Based on the focal macular cone ERGs in the cCSNB patients, we thought that the function of cone on-pathway may be preserved to some degrees in the central retina of the cCSNB patients. To test this hypothesis, it was necessary to record the focal macular cone ERGs from the monkey retina after the cone on-pathway was completely blocked pharmacologically by APB, and to compare these waveforms with those from cCSNB patients.

The focal macular cone ERGs recorded from two rhesus monkeys before and after intravitreous injection of APB are shown in Fig. 2. After the APB injection, the a-wave amplitude became larger, and the peak time of the a- and the following positive wave became prolonged. The d-wave was slightly enhanced after APB. The ratio of the b-wave to the a-wave amplitudes became smaller than controls, but was still larger than 1.0 (monkey #1, 1.24; monkey #2, 1.33).

We initially interpreted this to indicate that remaining positive wave might be caused by an incomplete blockage of APB and thus injected more APB. However, the addition of APB did not change the waveforms of the focal macular cone ERGs, and the b/a amplitude ratio still remained greater than 1.0 even after increasing the APB concentration to twice the original concentration (2 mM).

The similarity in the waveforms between cCSNB patients and monkeys treated with APB indicated that the cone on-pathway seemed be completely blocked even in the central retina in cCSNB.

3.3. Multifocal on- and off-responses in cCSNB and APB-treated monkey

We also noted that the waveforms of photopic ERG with long duration stimuli were different between full-field cone ERGs and focal macular cone ERGs in cCSNB patients; the amplitude of remaining positive wave was still larger than that of the a-wave, whereas the amplitude ratio of the positive wave to the a-wave was always less than 1.0 for the full-field ERGs (Fig. 1). However, these differences in the waveform could be due to the different stimulus and recording conditions in the two methods. Therefore, we next compared these waveforms between the central and peripheral retinas directly in a patient with cCSNB. For

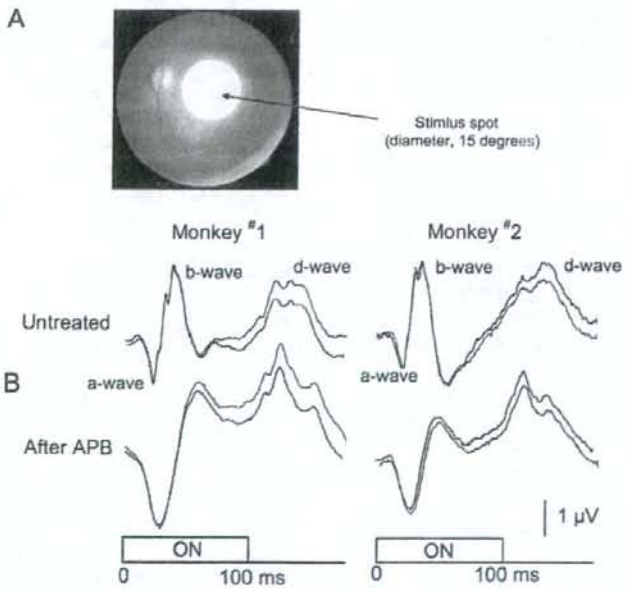

Fig. 2. Stimulus location and focal macular cone ERGs recorded from two monkeys. (A) Fundus photographs showing the stimulus spot. The 15° stimulus spot (diameter) was focused on the fovea. (B) Waveforms of focal macular cone ERGs before and after intravitreal injection of APB for two rhesus monkeys. Intravitreous concentration of APB was 1.0 mM.

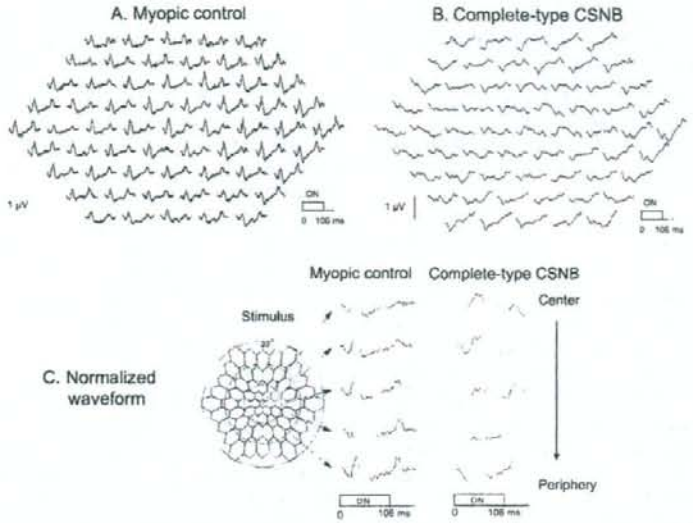

Fig. 3. Multifocal on- and off- responses using eight consequtive white frames. (A) Results from a myopic control. (B) Results from a patient with cCSNB (Case 1). (C) Normalized waveforms from five eccentric rings. Note that in cCSNB, the amplitude ratio of the positive wave to the a-wave is >1.0 in the central retina, but gradually become smaller towards to the periphery.

this purpose, we recorded the multifocal on- and off-responses (Kondo & Miyake, 2000; Kondo et al., 1998).

The multifocal on- and off-responses recorded from a representative myopic control (A), and a patient with cCSNB (B, Case 1 of Table 1) are shown in Fig. 3. It was clear that when compared to myopic control, the amplitudes of the positive wave are reduced at all locations in cCSNB. However, the amplitude of the positive wave is relatively preserved in the central retina, and the relative amplitude of the positive wave to the a-wave became small from the center to the periphery. The changes in the waveforms were clearly seen when the responses were grouped for each eccentric rings (Fig. 3C). The remaining positive wave is well preserved in the central retina, but gradually became smaller towards the peripheral retina. The amplitude ratio of the positive wave to the a-wave was >1.0 in the central retina, but <1.0 in the periphery. These findings are consistent with our combined findings of full-field ERG and focal macular cone ERGs in patients with cCSNB.

We also confirmed these results in a monkey retina after treatment with APB (Fig. 4). The remaining positive response was relatively large in the central retina, but the relative ratio of the positive wave to the a-wave gradually became smaller towards the periphery (Fig. 4C). These findings were quite similar to those in patients with cCSNB.

3.4. Origin of the remaining positive wave of photopic ERG at central retina

One question that still remained was the origin of the remaining positive component of the focal macular cone ERG seen even after blockage of cone on-pathway. To study the retinal origin of this component, we added PDA to block the neural activities of post-synaptic off-pathways and horizontal cells in monkeys. Fig. 5 shows the changes in the waveforms of photopic ERG with long duration stimulus before and after APB and PDA application for full-field and focal macular cone ERGs in a rhesus monkey. In this experiment, the same stimulus (30 cd/m^2) and background (3 cd/m^2) intensities were used for both full-field and focal macular cone ERGs, because the waveform of photopic ERG is dependent on the stimulus and background intensities (Kondo et al., 2000; Ueno, Kondo, Niwa, Terasaki, & Miyake, 2004). We found that after the PDA injection, the remaining positive wave of focal macular cone ERGs completely disappeared (lower traces of Fig. 5).

4. Discussion

We compared the waveform of focal macular cone ERGs recorded from cCSNB patients with those from APB-treated monkeys, and found that the waveforms were very similar: the amplitude of the a-wave was normal or slightly larger than control; a positive wave was still present after the a-wave, and the amplitude of this positive wave was larger than that of the a-wave; and the implicit time of the positive wave was delayed. These similarities in the waveform of focal macular ERG between the cCSNB patients and APB-treated monkeys suggested that the cone on-pathway is nearly completely blocked even in the central retina of the cCSNB patients.

Although the waveform of the a-wave and the following positive wave were very similar for cCSNB patients and